

We are IntechOpen, the world's leading publisher of Open Access books Built by scientists, for scientists

6,900

Open access books available

186,000

International authors and editors

200M

Downloads

Our authors are among the

154

Countries delivered to

TOP 1%

most cited scientists

12.2%

Contributors from top 500 universities



WEB OF SCIENCE™

Selection of our books indexed in the Book Citation Index
in Web of Science™ Core Collection (BKCI)

Interested in publishing with us?
Contact book.department@intechopen.com

Numbers displayed above are based on latest data collected.
For more information visit www.intechopen.com



Biosorption of Lanthanides Using Select Marine Biomass

Naoki Kano

Additional information is available at the end of the chapter

<http://dx.doi.org/10.5772/51164>

1. Introduction

Contamination of toxic metals in the aquatic environment is one of the most debated problems in the world with industrial development. Thus, the minimization and recovery of harmful pollutants such as heavy metals in natural environment is very significant [1]. Various treatment technologies such as ion exchange, precipitation, ultrafiltration, reverse osmosis and electrodialysis have been used for the removal of heavy metal ions from aqueous solution [2]. However, these processes have some disadvantages, such as high consumption of reagent and energy, low selectivity, high operational cost, and difficult further treatment due to generation of toxic sludge [3].

Among environmentally friendly technologies for the removal of heavy metals from aquatic effluent, biosorption has attracted increasing research interest recently [4-5]. The major advantages of biosorption are its high effectiveness in reducing the heavy metals and the use of inexpensive biosorbents [6]. Biosorption studies using various low cost biomass as adsorbents have been currently performed widely for the removal of heavy metals from aquatic effluent [7-18].

Among many biosorbents, marine seaweed can be an excellent biosorbent for metals because it is well known to concentrate metals [19-20]. Seaweeds are reported to accumulate hydrocarbons (as well as metals); and they are exposed to the ubiquitous presence of organic micropollutants and can work as suitable biomonitors [21]. Furthermore, it is considered that the shell (usually treated as waste material) can be also an promising adsorbent. The shell has an internal structure comprised of three distinct layers. The innermost layer (i.e., hypostracum) consists of aragonite; the middle layer (i.e., ostracum), which is the thickest of the three, consists of various orientations interbedded with protein molecules (conchiolin); and the outermost layer (i.e., periostracum) consists of chitin, which is represented as $(C_8H_{13}NO_5)_n$ [22]. Particularly, it is considered that protein (called

“conchiolin”) including amino acid group play an important role for collecting trace metal in shell [23].

Biosorption studies have been mainly focused on toxic elements such as Cd, Pb, Cu, As and Cr for subject elements [24]. In our research, the objective elements are mainly rare earth elements (REEs) from the viewpoint of resources recovery, although REEs do not represent a common toxic threat.

Rare earth elements (REEs) find wide range of applications as functional materials in agriculture and as other industrial products, then the demand of REEs in modern technology has increased remarkably over the past years [25-26]. These elements and their compounds have found a variety of applications especially in metallurgy, ceramic industry and nuclear fuel control [27]. For example, current applications of lanthanum as a pure element or in association with other compounds are in super alloys, catalysts, special ceramics, and in organic synthesis [28]. However, the shortage of trace metals including REEs (and the problem of stable supply for these metals) has been a concern in recent years. Therefore, the establishment of the removal or recovery method for trace metals is important from the viewpoint of resources recovery.

It is known that alginate is an exopolymer extracted mainly from brown algae (and various bacteria) that has been used both as immobilization material and as biosorbent of several heavy metals [29]. Then, biosorption studies using seaweed have been generally concentrated on brown algae so far [30-31]. Green and red algae as well as brown algae were also used for biosorbent of REEs in the present work.

Considering the above-mentioned, laboratory model experiments for confirming the efficiency of marine biomass (seaweed and shell) as sorbent for REEs was designed in present work. Furthermore, the surface morphology of the marine biomass used in this work was determined by SEM (Scanning Electron Microscope) before and after metal adsorption.

The crystal structure, and the specific surface area of the shell biomass were also determined by XRD (X-ray powder diffraction), and BET (Brunauer, Emmet and Teller) and Langmuir method, respectively.

2. Experimental work

2.1. Samples

The seaweed biomass

Many kinds of seaweeds samples (10 species of green algae, 21 species of brown algae and 21 species of red algae) were taken along several coasts in Niigata Prefecture (referred to the figure in our previous paper [32]) since April, 2004. Among seaweed species, the seaweeds for biosorbent used in this work were *Sargassum hemiphyllum* (brown algae), *Ulva pertusa* (green algae) and *Schizymenia dubyi* (red algae). Each seaweed sample was washed in the surrounding seawater to remove attachment at sampling place. After transport back to the

laboratory, the seaweed was first washed with tap water and ultrapure water thoroughly and then air-dried for 2-3 days. Afterwards, it was dried overnight in an electric drying oven (Advantec DRA 430DA) at maximum temperature of 55 °C to avoid degradation of the binding sites, the biomass was ground. Sizes of biomass ranging from 0.5 mm to 1 mm were obtained by passing through sieves (SANPO Test Sieves).

Based on Diniz and Volesky's study [31], each sieved biomass sample was loaded with Ca^{2+} in a solution of $50 \text{ mmol} \cdot \text{dm}^{-3} \text{ Ca}(\text{NO}_3)_2$ (biomass concentration of $10 \text{ g} \cdot \text{dm}^{-3}$) for 24 h under gentle agitation in order to remove the original cations on seaweed. Later, the biomass was washed with ultrapure water to remove excess Ca^{2+} until the mixture was reached approximately pH 5. Finally, the washed biomass was dried again overnight at 50°C in an electric drying oven, and stored in desiccators (containing silica gel as a desiccant) before use.

The shell biomass

Buccinum tenuissimum shellfish used for shell biomass were collected at fishermen's cooperative association. After being separated from the meat by boiling, organism shells were washed thoroughly with ultra-pure water after washed with tap water repeatedly. After drying, the shells were ground and sieved through a sieve (SANPO Test Sieves) to remove particles having size more than $500 \mu\text{m}$. Sieved material was used for adsorption experiments. Afterwards, a part of this sieved materials was heated for 6 h at 480°C or 950°C in an electric furnace (ISUZU Muffle Furnace STR-14K, Japan). Moreover, adequate ultrapure water was added to a part of heat-treatment (950°C, 6h) samples, and heated at 100 °C on a hotplate for evaporation to near dryness (removing water), and finally dried in an electric drying oven at 60 °C.

2.2. Sorption experiment for lanthanides using seaweed and shell biomass

The following sorption experiments were performed using the above-mentioned marine biomass. Experimental conditions (i.e., pH, contact time and biosorbent dose rate) in this work were optimized and determined based on our preliminary experiments [e.g., 21] and other literatures [24, 31]. The pH of each solution was adjusted by using $0.1 \text{ mol} \cdot \text{dm}^{-3} \text{ NH}_3\text{aq}$ / $0.1 \text{ mol} \cdot \text{dm}^{-3} \text{ HNO}_3$.

The seaweed biomass

Samples of 0.4 g of the biomass were contacted with 200 cm^3 of solution containing known initial each lanthanide (La, Eu or Yb) concentration ranging from 0.1 to $4 \text{ mmol} \cdot \text{dm}^{-3}$. Afterwards, the suspensions were shaken for 24 h in a water bath at ambient temperature ($\sim 25 \text{ }^\circ\text{C}$) at pH 4.

The shell biomass

Each sample of 0.2 g was contacted with 100 cm^3 of multi-element standard solution (prepared by XSTC-1) including known initial lanthanide concentration (10 to $500 \mu\text{g} \cdot \text{dm}^{-3}$)

in a 200 ml conical flask. Afterwards, the suspensions were shaken for 30 min in a water bath at room temperature at pH 5.

Following with each sorption experiment, the suspension containing biomass and lanthanides standard solution was filtered through a 0.10 μm membrane filter (Advantec Mixed Cellulose Ester, 47mm) to remove lanthanides that have been adsorbed into the biomass, and the concentration of these metals in the filtrate was determined with ICP-MS or ICP-AES.

The metal uptake by the marine biomass was calculated using the following mass balance equation [33]:

$$q = (C_i - C_f)V / W \text{ [mg} \times \text{g}^{-1}] \quad (1)$$

where q = metal uptake ($\text{mmol} \cdot \text{g}^{-1}$); C_i = initial metal concentration ($\text{mmol} \cdot \text{dm}^{-3}$); C_f = equilibrium metal concentration ($\text{mmol} \cdot \text{dm}^{-3}$); V = volume of the solution (dm^3); and W = dry mass of seaweed (g).

The removal efficiency (RE, %) of the biosorbent on the metal in the solution was determined by the following equation [24]:

$$RE = (C_i - C_f) \times 100 / C_i \quad (2)$$

2.3. Langmuir and Freundlich isotherm model

Langmuir adsorption isotherm model was applied based on Tsui et al. [24] in this study, and the model assumes monolayer sorption onto a surface and is given as below.

$$q = (q_e \times C_f) / (A^{-1} + C_f) \quad (3)$$

where q_e = maximum metal uptake ($\text{mmol} \cdot \text{g}^{-1}$) (i.e., the maximum attainable binding capacity); and A = affinity constant (1 mmol^{-1}) (i.e., the affinity of the metal ion toward the biomass).

The Freundlich equation is widely used in the field of environmental engineering, and was applied based on based Dahiya et al. [10-11]. Freundlich isotherm can also be used to explain adsorption phenomenon as given below.

$$\log_{10} q_e = \log_{10} K_F + (1/n) \log_{10} C_f \quad (4)$$

where K_F and n are constants incorporating all factors affecting the adsorption capacity and an indication of the favorability of metal ion adsorption onto biosorbent, respectively. It is shown that $1/n$ values between 0.1 and 1.0 correspond to beneficial adsorption. That is, q_e versus C_f in log scale can be plotted to determine values of $1/n$ and K_F .

3. Results and discussion

3.1. The seaweed samples

3.1.1. Metal sorption capacity at different species of seaweed

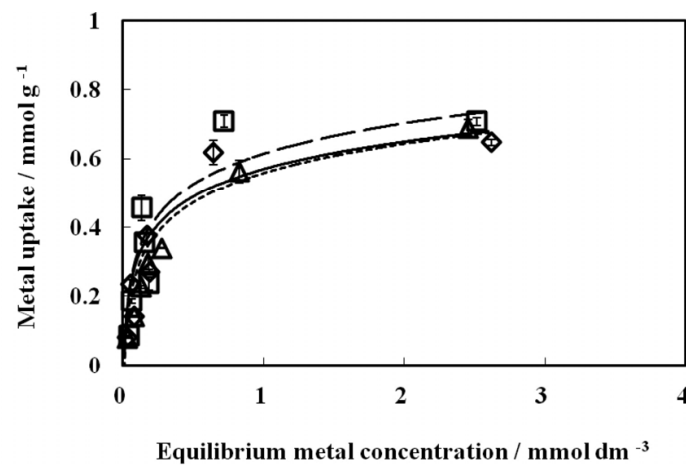
The equilibrium sorption isotherms of La, Eu and Yb by three kinds of Ca-loaded seaweed biomass are shown in Fig. 1. Sorption experiment of Eu using *U.p.* could not be conducted in this work due to the lack of sample. The adsorption data obtained in this work were analyzed using Langmuir and Freundlich equations. The correlation coefficients (R^2) of Langmuir and Freundlich isotherms for La, Eu and Yb using three kinds of seaweed biomass are shown in Table 1 along with other parameters.

From this table, it is found that R^2 value for each datum is comparatively large for both isotherms. The value of $1/n$ less than unity indicates better adsorption and formation of relatively stronger bonds between adsorbent and adsorbate [10]. That is to say, favorable adsorption for La, Eu and Yb by these seaweed biomass used in this work is presented. Furthermore, it is noted that R^2 values for these data are particularly large for Langmuir isotherm than for Freundlich isotherm. This result suggests that the adsorption on these samples mainly occurred by monolayer reaction. Therefore, the curves obtained from non-linear regression of the data by Langmuir isotherm are also shown in Fig. 1.

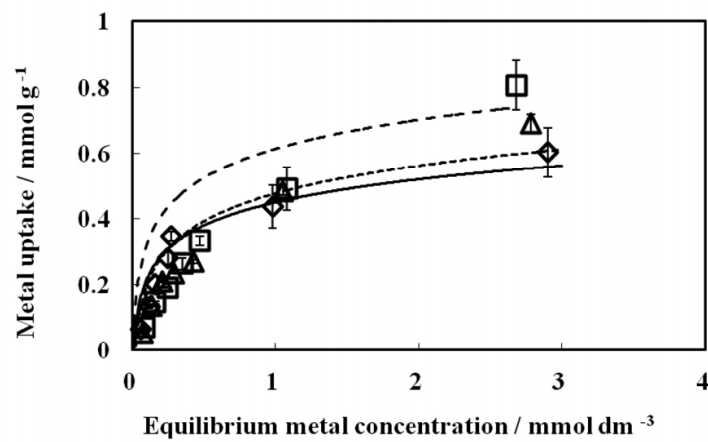
	<i>Sargassum hemiphyllum</i>			<i>Schizymenia dubyi</i>			<i>Ulva pertusa</i>		
	La	Eu	Yb	La	Eu	Yb	La	Eu	Yb
Langmuir									
$q_e / \text{mmol g}^{-1}$	0.700	0.781	0.769	0.651	0.980	0.926	0.930	---	0.719
A / mmol^{-1}	5.19	4.33	3.03	2.53	1.05	1.08	6.03	---	1.59
R^2	0.992	0.987	0.999	0.982	0.969	0.983	0.996	---	0.991
Freundlich									
K_F / g^{-1}	0.575	0.648	0.561	0.450	0.475	0.443	0.816	---	0.409
$1/n$	0.440	0.462	0.500	0.531	0.683	0.646	0.461	---	0.595
R^2	0.806	0.731	0.937	0.839	0.969	0.923	0.878	---	0.923

Table 1. Langmuir and Freundlich parameters for biosorption of lanthanides on three kinds of Ca-loaded biomass at pH 4.0 (--- represents the missing data due to the lack of sample)

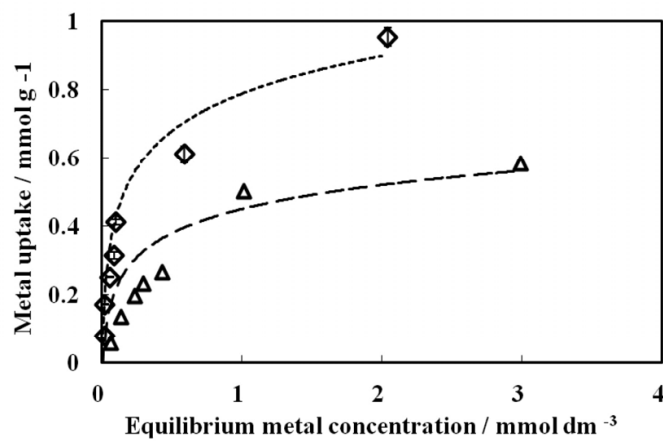
From Table 1, it is found that the data of q_e for Eu and Yb by *Sargassum hemiphyllu* (brown algae) obtained in this study are similar to the result of species of *Sargassum* conducted by Diniz and Volesky [31], although q_e for La is slightly small. Moreover, it is noteworthy that both Langmuir parameters: q_e and A for La by *Ulva pertusa* (green algae) is large. Then, the comparison of sorption isotherms of La among three kinds of seaweed biomasses is shown in Fig. 2. From this figure, the sorption capacity of La by *U. p.* (green algae) is considerably large compared to that by other algae: *S. h.* (brown algae) and *S. d.* (red algae). It is generally known that brown seaweed is superior to red and green seaweed in metal sorption capacity for heavy metals such as Cd, Pb, Cu [34-35]; and such a high value



(a)



(b)



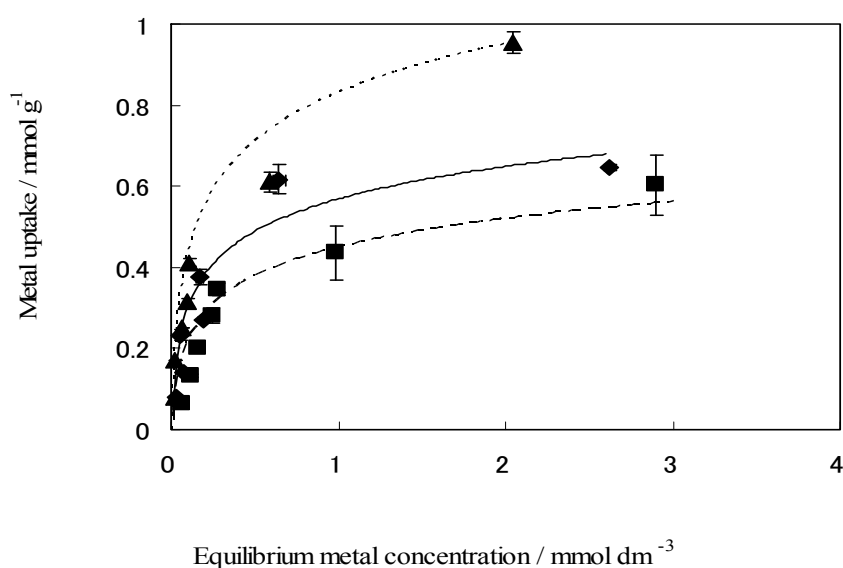
(c)

Figure 1. Sorption isotherms of La (\diamond), Eu (\square) and Yb (Δ) by three kinds of Ca-loaded seaweed biomass at pH 4.0, (a): *Sargassum hemiphyllum*, (b): *Schizymenia duby* and (c): *Ulva pertusa*. The curves obtained from non-linear regression of the data by Langmuir isotherm are also shown (La: solid curve, Eu: broken curve and Yb: dotted curve). Data are mean \pm standard deviation ($n=3$).

of q_e (as observed in this work) using green algae have not been reported so far. In other words, it is significant outcome to find that *Ulva pertusa* (green algae) can be a promising biosorbent for removing La.

According to our previous work [32], in case of U, the mean concentration is the highest in brown algae and is the lowest in green algae among phyla (i.e., green, red and brown algae). However, as for the mean concentration of light REE (LREE) such as La, a slightly higher concentration is found in green algae; whereas the concentration of heavy REE (HREE) such as Yb or Lu in green algae is smaller than that in brown algae (as shown in the figure in our previous paper [32]).

Then, large sorption capacity of La by *Ulva pertusa* may be related to the character (or the constituent) of green algae; and it is possible that “La adsorption on *Ulva pertusa*” is due to “metal-specific”, although further studies is needed to confirm the peculiarity by investigating the other combinations of metals and seaweed species.



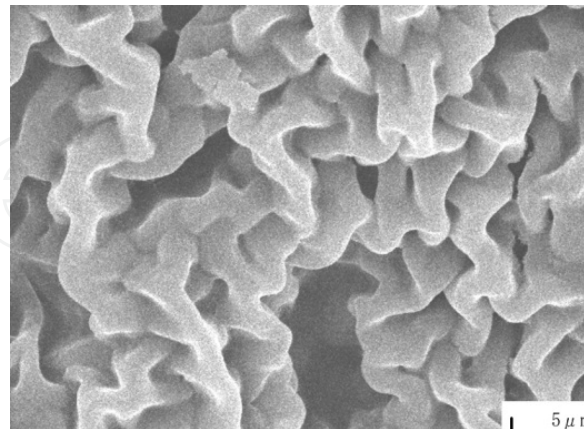
◆ : *Sargassum hemiphyllum*, ■ : *Schizymenia duby*, ▲ *Ulva pertusa*. The curves obtained from non-linear regression of the data by Langmuir isotherm are also shown (*S. h.*; solid curve, *S. d.*; broken curve and *U. p.*; dotted curve). Data are mean±standard deviation (n=3).

Figure 2. Comparison of sorption isotherms for La among three kinds of Ca-loaded seaweed biomass at pH 4.0

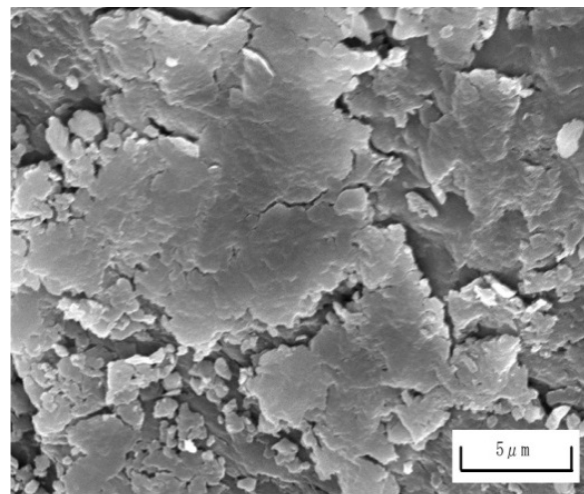
SEM pictures of three kinds of Ca-loaded seaweed biomass before and after adsorption of lanthanum are shown in Fig. 3 and Fig. 4, respectively.

According to SEM observation, the surface of *S. d.* (red algae) seems to be relatively flat, whereas *S. h.* (brown algae) and *U. p.* (green algae) have more extensive surface area, although the specific surface area of the seaweed biomass could not be measured due to their small specific surface area. Furthermore, by comparing SEM pictures in Fig. 3 with that in Fig. 4, it is found that the morphology of *S. h.* and *U. p.* surface has hardly changed even

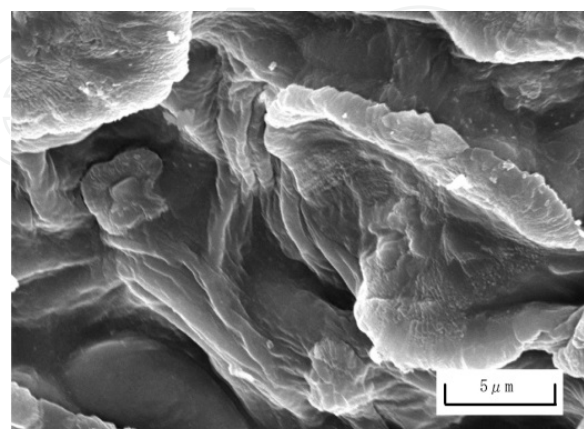
after exposing lanthanum. On the other hand, the distinct change of the surface morphology on *S. d.* was observed after adsorption of metals.



(a)

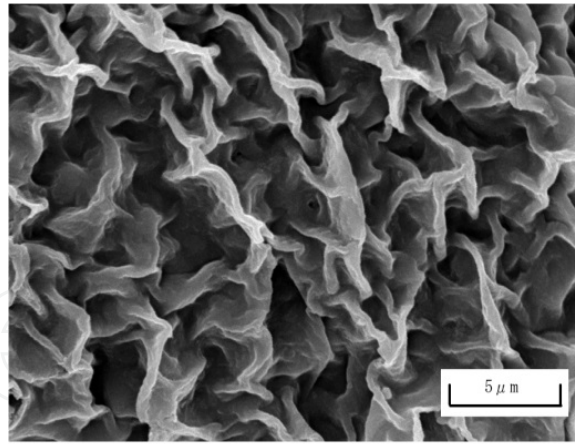


(b)

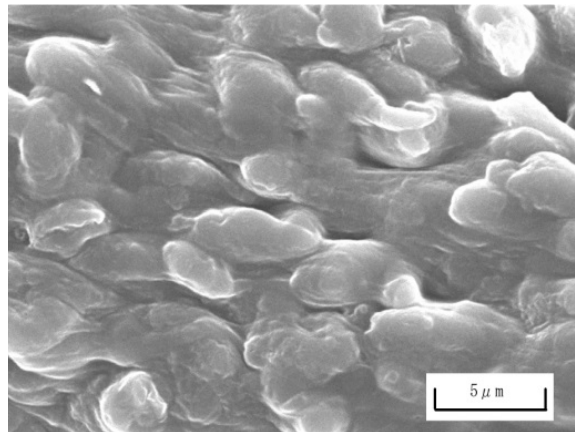


(c)

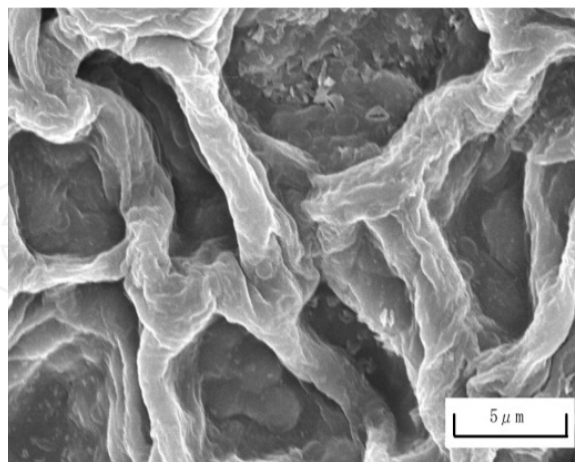
Figure 3. SEM pictures of seaweed biomass before adsorption of lanthanum. (a) : *Sargassum hemiphyllum*. (b) *Schizymenia duby* and (c) : *Ulva pertusa*.



(a)



(b)



(c)

Figure 4. SEM pictures of seaweed biomass after adsorption of lanthanum. (a) : *Sargassum hemiphyllum*. (b) *Schizymenia duby* and (c) : *Ulva pertusa*.

From the above observation, two kinds of biomass: *Sargassum hemiphyllum* and *Ulva pertusa* should be predicted to withstand the repeated use; and hence it can be a good adsorbent for lanthanides.

3.1.2. Removal efficiency and binding mechanism of seaweed biomass

The removal efficiency (RE) of 3 kinds of seaweed biomass as a function of initial metal concentrations (C_i) for 3 lanthanides is shown in Fig. 5((a): La, (b): Eu, (c): Yb). With increasing C_i , the RE generally decreased exponentially; and at high C_i , similar RE (i.e., about 40%) occurred for each lanthanide even with any biomass. These data are well fitted into an exponential function (R^2 ranging from 0.866 to 0.994) shown in Fig. 5; and the equations and R^2 for each lanthanide in each biomass are shown in Table 2.

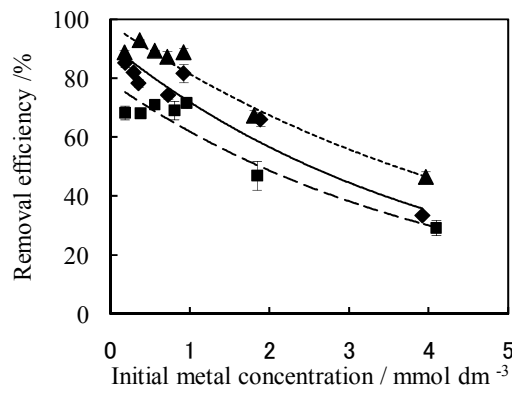
From the viewpoint of recovering trace metals from aqueous environment such as seawater, the removal efficiency at low concentration of metal is particularly important. The coefficient before exponential function in each equation in Table 2 represents the value of RE at low C_i near approximately zero $\text{mmol}\cdot\text{dm}^{-3}$. From Table 3, the coefficient for each lanthanide in *Sargassum hemiphyllum* and especially that for La in *Ulva pertusa* is large. This implies that *U. p.* could be an efficient adsorbent for La as well as *S. h.* for lanthanides in aqueous environment such as seawater.

The amount ($\text{mmol}\cdot\text{g}$) of adsorbed lanthanide and released Ca from three kinds of Ca-loaded seaweed biomass is shown in Tables 3-5. Based on the data in these tables, relationship between the uptake of each lanthanide ion and calcium ion released from each biomass is shown both in terms of mill equivalent per gram ($\text{meq}\cdot\text{g}^{-1}$) in Fig. 6. Good and linear relationship is generally found for these samples between the uptake of each lanthanide and Ca released from these biomasses into the solution as shown in Fig. 6. Particularly, in case of *S. h.* and *U. p.*, the slope of the line is about one with the y-intercept of the graphs almost passes through the origin. It indicates that ion-exchange process is found to be the main mechanism responsible for the sorption of lanthanide ion onto the seaweed as Tsui et al. [24] and Diniz & Volesky [31] also pointed out.

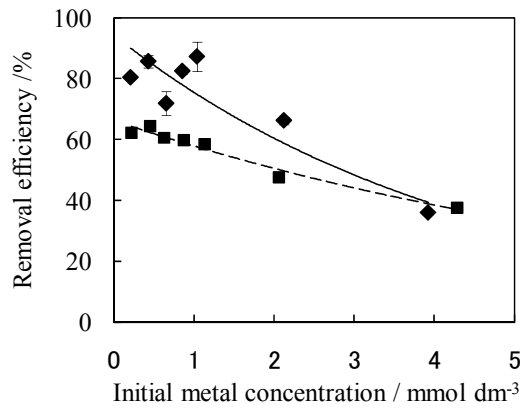
	<i>Sargassum hemiphyllum</i>		<i>Schizymenia dubyi</i>		<i>Ulva pertusa</i>	
	Equation	R^2	Equation	R^2	Equation	R^2
La	$\text{RE}=91.4\exp(-0.239C_i)$	0.939	$\text{RE}=78.7\exp(-0.241C_i)$	0.939	$\text{RE}=98.5\exp(-0.191C_i)$	0.993
Eu	$\text{RE}=94.3\exp(-0.223C_i)$	0.866	$\text{RE}=66.2\exp(-0.136C_i)$	0.973	-----	---
Yb	$\text{RE}=88.9\exp(-0.234C_i)$	0.994	$\text{RE}=68.2\exp(-0.173C_i)$	0.944	$\text{RE}=70.3\exp(-0.213C_i)$	0.975

--- represents the defect of data due to the lack of sample

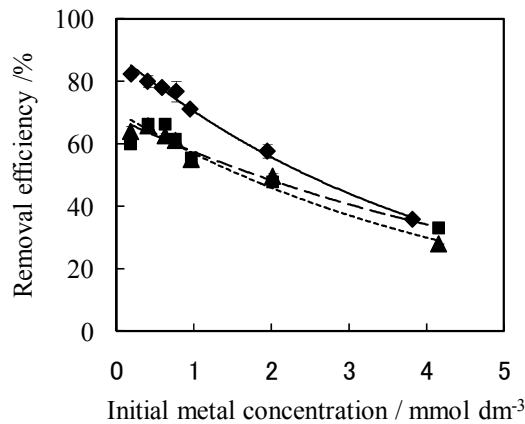
Table 2. Equations and correlation coefficients (R^2) to describe the relationships between removal efficiency (RE) and initial concentrations (C_i) of different lanthanides in the sorption system



(a)



(b)



(c)

Figure 5. Removal efficiency of lanthanides ((a) :La, (b) :Eu, (c) :Yb) by Ca-loaded seaweed biomass at different initial concentrations, \blacklozenge : *Sargassum hemiphyllum*, \blacksquare : *Schizymeria duby*, \blacktriangle : *Ulva pertusa*. Each exponential function is also shown (*S. h.*; solid curve, *S. d.* : broken curve and *U. p.* : dotted curve). Data are mean \pm standard deviation (n=3).

3.2. The shell samples

3.2.1. Characteristics of *Buccinum tenuissimum* shell biomass

<i>Sargassum hemiphyllum</i>				
	Adsorbed lanthanide / mmol g ⁻¹	Total Released Ca / mmol g ⁻¹	Ca excess (blank) / mmol g ⁻¹	Net Released Ca / mmol g ⁻¹
La	0.081	0.208	0.082	0.126
	0.121	0.226	0.082	0.144
	0.150	0.276	0.082	0.194
	0.153	0.305	0.082	0.224
	0.234	0.507	0.082	0.426
	0.375	0.595	0.082	0.514
	0.617	0.995	0.082	0.913
	Eu	0.085	0.155	0.080
0.186		0.298	0.080	0.218
0.237		0.377	0.080	0.297
0.355		0.576	0.080	0.496
0.456		0.791	0.080	0.711
0.707		1.021	0.080	0.941
0.708		1.507	0.080	1.427
Yb		0.079	0.194	0.077
	0.160	0.288	0.077	0.211
	0.227	0.403	0.077	0.326
	0.296	0.494	0.077	0.417
	0.339	0.579	0.077	0.502
	0.563	0.838	0.077	0.761
	0.688	0.958	0.077	0.881

Table 3. Amount of adsorbed lanthanide and released Ca by Ca-loaded *Sargassum hemiphyllum* biomass

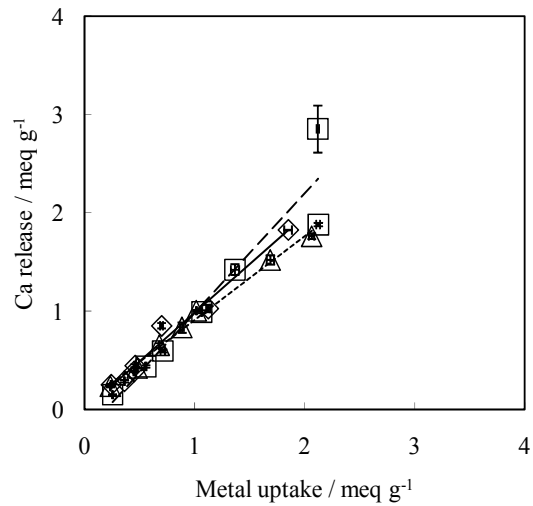
X-ray powder diffraction (XRD) patterns of the four kinds of *Buccinum tenuissimum* shell biomass samples are shown in Fig. 7. The crystal structure of the shell biomass was transformed from aragonite (CaCO₃) into calcite (CaCO₃) phase by heat-treatment (480°C, 6h). Moreover, the crystal structure of the shell biomass was mainly transformed into calcium oxide (CaO) by heat-treatment (950°C, 6h); and was mainly into calcium hydroxide (Ca(OH)₂) by adding water after heat-treatment (950°C, 6h). SEM pictures of the four kinds of sieved shell biomass samples are shown in Fig. 8. Comparing Fig. 8(b) with Fig. 8(a), comparatively clear crystal with a lot of big particles may be observed by heat-treatment (480°C, 6h). It is suggested that ground original sample contains a lot of organic materials such as protein, and most of organic matter seem to disappear by heat-treatment. Moreover, fine crystal particle is not observed in Fig. 8 (c). This may be attributable to the phenomena that many crystals were connected largely with each other due to high-temperature sintering. Meanwhile, relative clear crystal (sizes are mostly 1.0-4.0µm) is observed in Fig. 8 (d).

<i>Schizymenia dubyi</i>				
	Adsorbed lanthanide / mmol g ⁻¹	Total Released Ca/ mmol g ⁻¹	Ca excess (blank) / mmol g ⁻¹	Net Released Ca / mmol g ⁻¹
La	0.053	0.376	0.240	0.136
	0.132	0.469	0.240	0.229
	0.201	0.571	0.240	0.331
	0.281	0.657	0.240	0.417
	0.346	0.747	0.240	0.507
	0.436	0.757	0.240	0.517
	0.603	0.835	0.240	0.595
Eu	0.070	0.655	0.240	0.415
	0.146	0.778	0.240	0.538
	0.192	0.862	0.240	0.622
	0.263	1.025	0.240	0.785
	0.333	1.176	0.240	0.936
	0.493	2.102	0.240	1.862
	0.807	2.146	0.240	1.906
Yb	0.055	0.557	0.240	0.317
	0.136	0.594	0.240	0.354
	0.210	0.694	0.240	0.454
	0.236	0.796	0.240	0.556
	0.270	0.771	0.240	0.531
	0.483	0.950	0.240	0.710
	0.691	1.036	0.240	0.796

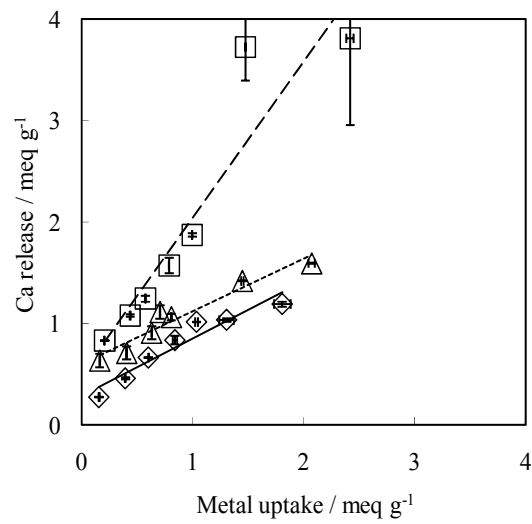
Table 4. Amount of adsorbed lanthanide and released Ca by Ca-loaded *Schizymenia dubyi* biomass

<i>Ulva pertusa</i>				
	Adsorbed lanthanide / mmol g ⁻¹	Total Released Ca/ mmol g ⁻¹	Ca excess (blank) / mmol g ⁻¹	Net Released Ca / mmol g ⁻¹
La	0.079	0.259	0.160	0.099
	0.172	0.314	0.160	0.154
	0.251	0.415	0.160	0.255
	0.315	0.658	0.160	0.498
	0.412	0.776	0.160	0.616
	0.610	1.546	0.160	1.386
	0.929	1.672	0.160	1.512
Yb	0.059	0.263	0.160	0.103
	0.134	0.349	0.160	0.189
	0.198	0.449	0.160	0.289
	0.234	0.644	0.160	0.484
	0.266	0.704	0.160	0.544
	0.503	1.132	0.160	0.972
	0.584	1.421	0.160	1.261

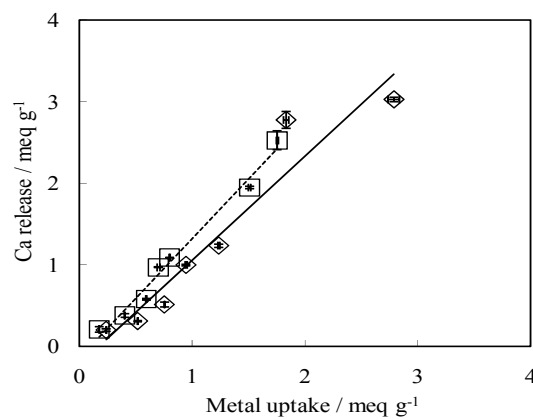
Table 5. Amount of adsorbed lanthanide and released Ca by Ca-loaded *Ulva pertusa* biomass



(a)

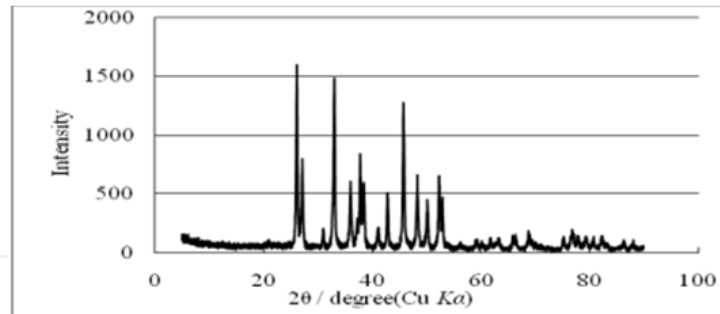


(b)

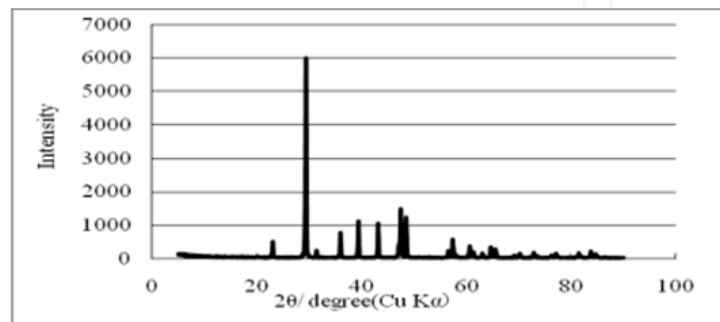


(c)

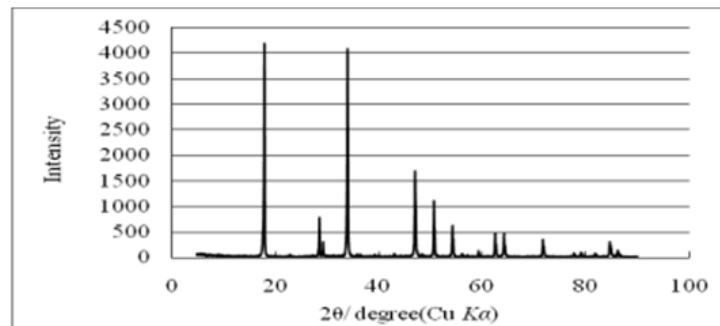
Figure 6. Relationship between metal uptake and Ca release from Ca-loaded seaweed biomass, (a): *Sargassum hemiphyllum*, (b): *Schizymenia duby* and (c): *Ulva pertusa*. \diamond :La, \square :Eu, \triangle :Yb. Each regression line is also shown (La: solid line, Eu: broken line and Yb: dotted line). Data are mean \pm standard deviation (n=3).



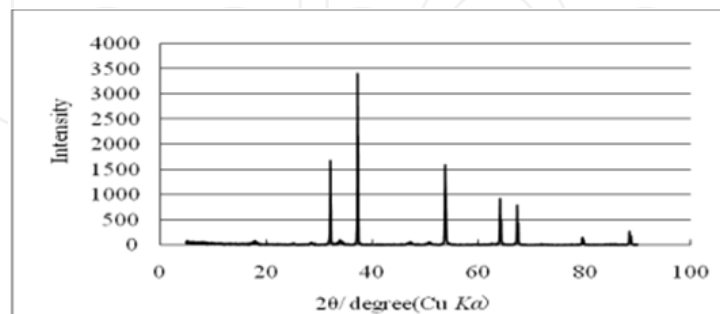
(a)



(b)



(c)



(d)

Figure 7. X-ray diffraction (XRD) patterns of *Buccinum tenusimum* shell biomass before adsorption of metals. (a) ground original sample, (b) heat-treatment (480 °C) sample, (c) heat-treatment (950 °C) sample, (d) heat-treatment (950 °C) and water added sample.

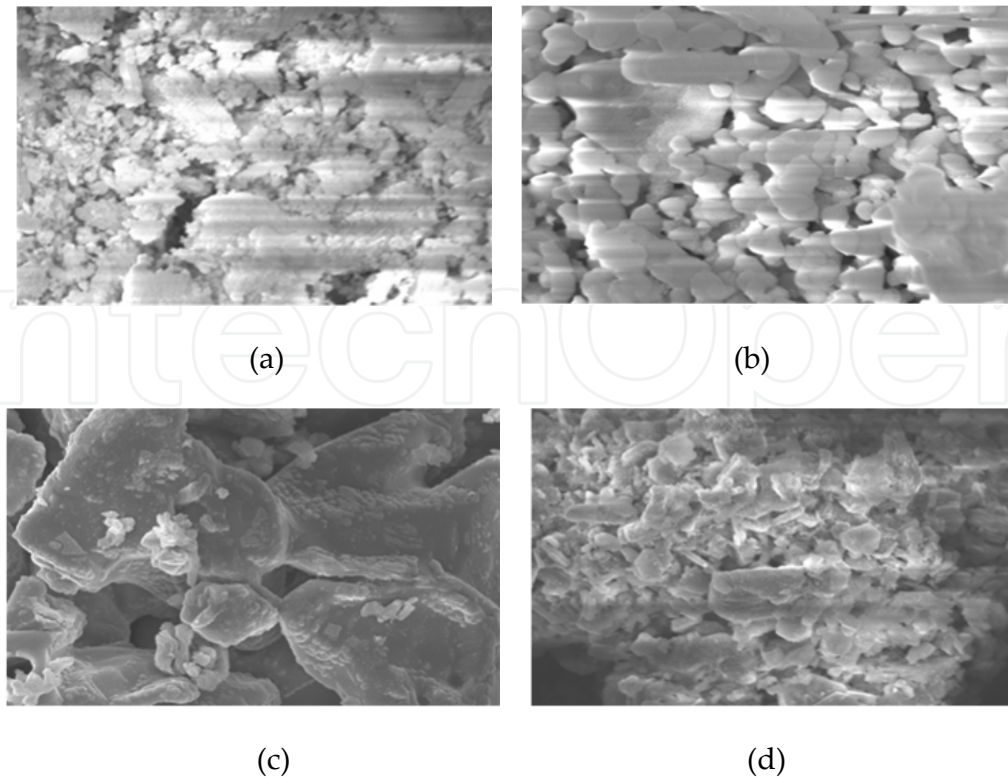


Figure 8. SEM pictures of *Buccinum tenuissimum* shell biomass before adsorption of metals. (a) ground original sample, (b) heat-treatment (480°C) sample, (c) heat-treatment (950°C) sample, (d) heat-treatment (950°C) and water added sample

Furthermore, the measurement of specific surface area of the four kinds of sieved samples was performed in this study; and the results are shown in Table 6 along with the main crystal structure of these samples. Remarkably decrease of specific surface area (i.e., from 3.32m²/g to 0.390m²/g for BET, or from 5.35 m²/g to 0.612 m²/g for Langmuir) was found after heat-treatment (480°C, 6h). It is suggested that the crystal structure transformation (i.e., from aragonite (CaCO₃) into calcite (CaCO₃) phase) and also the difference of the surface morphology can be closely related to the remarkable decrease of specific surface area of the shell biomass. On the other hand, the surface area of “heat-treatment (950°C, 6h) sample” was 1.88m²/g for BET or 3.10m²/g for Langmuir respectively; and that of “heat-treatment (950°C, 6h) and water added sample” was 6.37m²/g for BET or 9.91m²/g for Langmuir, respectively.

3.2.2. Comparison for sorption capacity of lanthanides by four kinds of sieved biomass

The comparison for sorption capacity of lanthanides by four kinds of sieved *Buccinum tenuissimum* shell samples is shown in Fig. 9. In this experiment, the initial lanthanides concentration was taken as 100μg·dm⁻³. From this figure, it is found that all kinds of sieved samples showed excellent sorption capacity under this experimental condition. However, the sorption capacity in sample (b) (i.e., the main phase is calcite) decreases slightly relative to that of the original material (i.e., (a): the main phase is aragonite) and others. The decrease

Sample	Main crystal structure	Specific surface area
(a) Ground original sample	Aragonite (CaCO ₃)	3.31m ² /g (BET) 5.35m ² /g (Langmuir)
(b) Heat-treatment (480°C) sample	Calcite (CaCO ₃)	0.390m ² /g (BET) 0.612m ² /g (Langmuir)
(c) Heat-treatment (950°C) sample	Lime syn. (CaO)	1.88m ² /g (BET) 3.10m ² /g (Langmuir)
(d) Heat-treatment (950°C) and water added sample	Portlandite (Ca(OH) ₂)	6.37m ² /g (BET) 9.91m ² /g (Langmuir)

Table 6. The crystal structures and the specific surface areas of four kinds of sieved *Buccinum tenuissimum* shell biomass

of sorption capacity in sample (b) may be attributable to the remarkable decrease (i.e., by a factor of less than one eighth) of specific surface area of the biomass.

Prieto et al. [36] pointed that the sorption capacity of calcite is considerably lower than that of aragonite for Cd. In case of lanthanides, similar tendency of sorption capacity were suggested from our work.

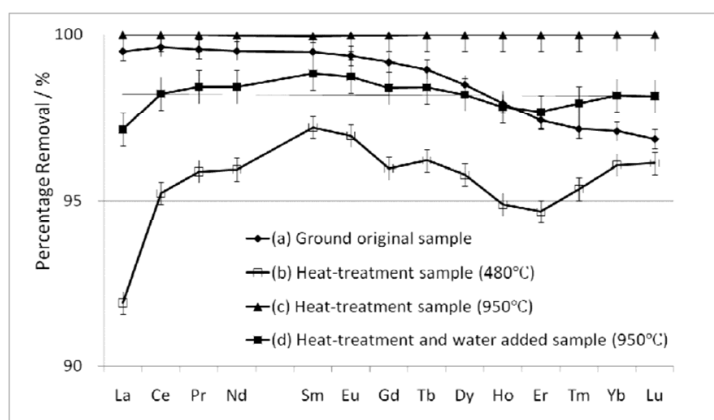


Figure 9. Comparison for sorption capacity of lanthanides by four kinds of sieved *Buccinum tenuissimum* shell samples.

3.2.3. Effect of competitive ions on the sorption of lanthanides

The percentage removal of lanthanides under the presence of common ions (Ca²⁺, Mg²⁺, Na⁺ and K⁺) at different concentrations 50, 100 and 200 mg·dm⁻³ is shown in Fig. 10. From this figure, the remarkable decrease of sorption capacity of lanthanides was not observed. Even when the concentrations of common ions are 200 mg·dm⁻³, the percentage removal of light REE (LREE) such as La or Ce decreased slightly (2-3%), whereas the removal decreased about 5% for heavy REE (HREE) such as Yb or Lu. This implies that the shell biomass can be an efficient adsorbent for lanthanides in aqueous environment such as seawater, although it requires further investigations to apply the shell biomass to use as an adsorbent for lanthanides more practically.

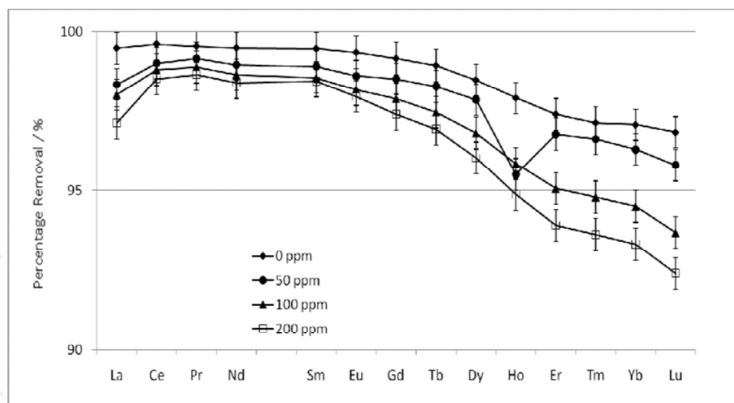


Figure 10. Effect of common ions (Ca^{2+} , Mg^{2+} , Na^+ and K^+) on the removal efficiency of lanthanides using ground original sample.

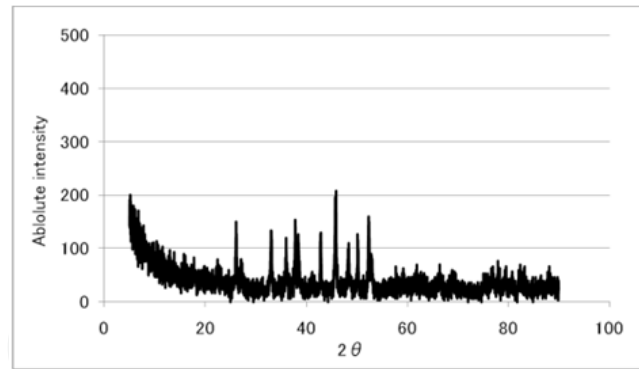
3.2.4. Characteristics of *Buccinum tenuissimum* shell biomass after adsorption of metals

X-ray diffraction (XRD) patterns of four kinds of sieved samples after adsorption of metals are shown in Fig. 11. Similar to the XRD patterns before adsorption of metals, aragonite and calcite were found as the main crystal structure in (a): Ground original sample and (b): Heat-treatment (480°C , 6h) sample, respectively. However, the decrease of peak and increase of noise were also observed in both patterns, particularly in the ground original material as shown in Fig. 11(a). Bottcher [37] pointed out that the natural powdered aragonite was transformed to mixed rhombohedral carbonates by the reaction with (Ca, Mg)-chloride solutions. Therefore, there is the possibility that the transformation of aragonite occurred by the reaction with lanthanides in our experiment.

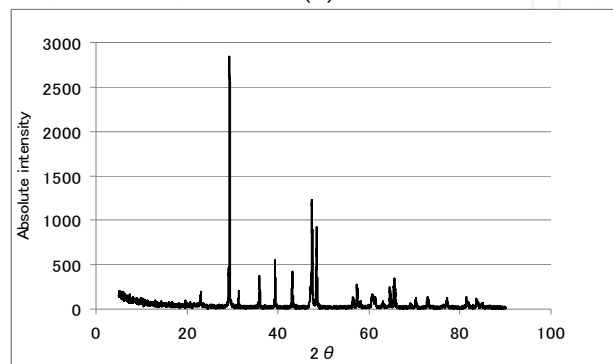
Moreover, according to XRD analysis, the main crystal structure of (c): “Heat-treatment (950°C) sample” was transformed from calcium oxide (CaO) to the mixture of calcium hydroxide ($\text{Ca}(\text{OH})_2$) and calcite (CaCO_3) after exposing metals; and that of (d): “Heat-treatment (950°C) and water added sample” was transformed from calcium hydroxide ($\text{Ca}(\text{OH})_2$) to calcite (CaCO_3) after adsorption of metals. These changes may be due to the reaction with water or carbon dioxide in atmosphere.

SEM pictures of four kinds of shell biomass after adsorption of metals are shown in Fig. 12. By comparing SEM pictures in Fig. 8 with that in Fig. 12, it is found that the morphology of sample (a) and (b) has hardly changed even after exposing metals. From this observation, these sieved samples should be predicted to withstand the repeated use; and hence it can be a good adsorbent.

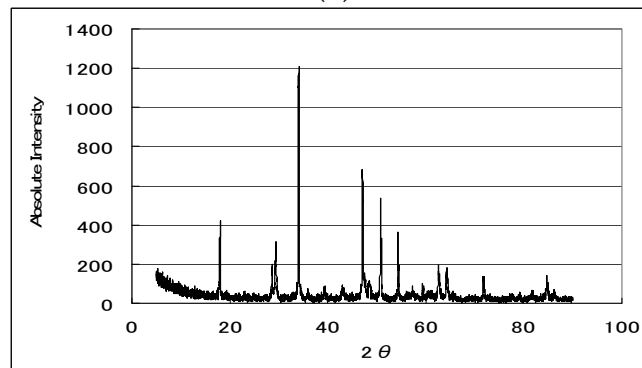
In contrast to sample (a), clear crystal structure (sizes are mostly $0.25\text{-}2.0\mu\text{m}$) was observed in sample (b) even after adsorption of metal. In case of Cd conducted by Kohler et al. [38], the difference of procedure for reaction with metals between aragonite and calcite was suggested. According to their work, the precipitation of several distinct types of crystals was observed after exposing metals in the case of aragonite. Then, it is anticipated that similar phenomenon were occurred by adsorption of lanthanides in case of our samples. On the



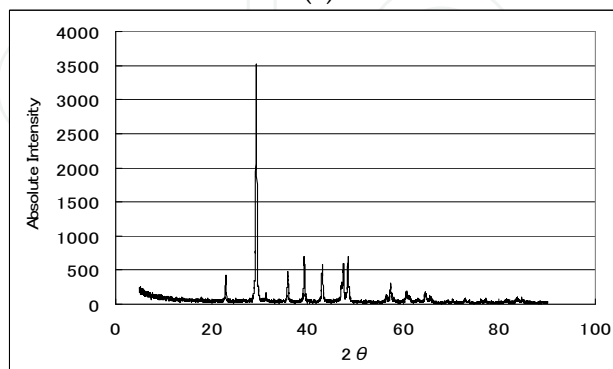
(a)



(b)



(c)



(d)

Figure 11. X-ray diffraction (XRD) patterns of *Buccinum tenussimum* shell biomass after adsorption of metals. (a) ground original sample, (b) heat-treatment (480°C) sample, (c) heat-treatment (950°C) sample, (d) heat-treatment (950°C) and water added sample

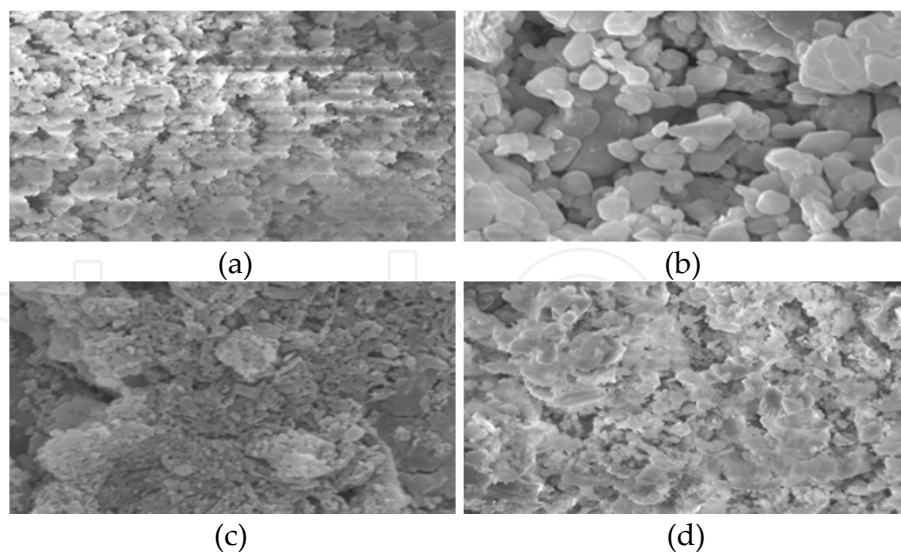


Figure 12. SEM pictures of *Buccinum tenuissimum* shell biomass after adsorption of metals. (a) ground original sample, (b) heat-treatment (480°C) sample, (c) heat-treatment (950°C) sample, (d) heat-treatment (950°C) and water added sample

other hand, the surface of sample (c) and (d) after exposing metals have changed largely compared to that before adsorption of metals (Fig. 8). This is in good accord with the results of XRD patterns. Particularly, remarkable transformation was observed in the morphology of sample (d). The reaction of sample (d) with metal is supposed to proceed rapidly.

3.2.5 Adsorption isotherms of lanthanides by *Buccinum tenuissimum* shell biomass

The adsorption data obtained for lanthanides using *Buccinum tenuissimum* shell biomass were analyzed using Langmuir and Freundlich equations. The correlation coefficient (R^2) of Langmuir and Freundlich isotherms for lanthanides using ground original shell biomass is shown in Table 7 along with other relevant parameters.

From this table, it is found that R^2 value for lanthanides is comparatively high. It indicates the applicability of these adsorption isotherms satisfactorily for lanthanides in this sample. The dimensionless parameter Hall separation factor (R_L) for lanthanides is in the range of $0 < R_L < 1$, which means that the sorption for lanthanides by this shell biomass is favorable. Furthermore, the negative value of ΔG indicates that the sorption is spontaneous. The higher R^2 value for Freundlich model rather than for Langmuir isotherm (0.638-0.886 for Langmuir isotherm and 0.844-0.932 for Freundlich one) suggests that the adsorption on this sample is due to multilayer coverage of the adsorbate rather than monolayer coverage on the surface. It is noted that the value of $1/n$ less than unity indicates better adsorption mechanism and formation of relatively stronger bonds between adsorbent and adsorbate [10]. That is to say, favorable adsorption for lanthanides by this shell biomass is presented.

On the other hand, R^2 and other parameters of Langmuir and Freundlich isotherms for lanthanides using “heat-treatment (480°C) sample” is shown in Table 8. It is noteworthy that R^2 value for REEs in this sample is still more large (0.947-0.982 for Langmuir isotherm and 0.948-0.975 for Freundlich one), compared with the original ground sample (Table 7).

	Langmuir				Freundlich			
	a	b	R^2	$\Delta G_{\text{ads}}/$ kJmol^{-1}	R_L	K_F	$1/n$	R^2
La	400	0.490	0.638	-15.3	0.0200	115	0.654	0.844
Ce	370	1.17	0.886	-17.5	0.0084	163	0.583	0.864
Pr	400	0.714	0.750	-16.3	0.0138	145	0.658	0.853
Nd	400	0.610	0.681	-15.9	0.0161	133	0.662	0.846
Sm	417	0.632	0.740	-16.0	0.0156	145	0.709	0.863
Eu	417	0.571	0.794	-15.7	0.0172	136	0.723	0.883
Gd	435	0.418	0.788	-15.0	0.0234	114	0.765	0.904
Tb	476	0.328	0.800	-14.4	0.0296	105	0.778	0.912
Dy	476	0.239	0.849	-13.8	0.0367	81.8	0.804	0.932
Ho	476	0.183	0.870	-12.9	0.0519	65.2	0.799	0.924
Er	476	0.148	0.878	-12.4	0.0633	55.6	0.787	0.920
Tm	476	0.135	0.842	-12.2	0.0687	52.6	0.785	0.910
Yb	476	0.136	0.818	-12.2	0.0683	53.3	0.762	0.887
Lu	500	0.119	0.786	-11.8	0.0775	51.3	0.759	0.877

Table 7. Coefficient of Langmuir and Freundlich isotherms for lanthanides using original *Buccinum tenuissimum* shell biomass

	Langmuir				Freundlich			
	a	b	R^2	ΔG_{ads} kJmol^{-1}	R_L	K_F	$1/n$	R^2
La	192	0.243	0.982	-13.6	0.0395	57.2	0.258	0.948
Ce	278	0.234	0.972	-13.5	0.0410	70.4	0.292	0.956
Pr	303	0.229	0.962	-13.5	0.0418	71.5	0.321	0.955
Nd	313	0.225	0.956	-13.4	0.0425	72.5	0.328	0.954
Sm	345	0.266	0.948	-13.8	0.0362	78.4	0.359	0.962
Eu	345	0.248	0.947	-13.7	0.0388	76.0	0.364	0.963
Gd	303	0.231	0.955	-13.5	0.0415	75.0	0.299	0.954
Tb	323	0.221	0.961	-13.4	0.0432	69.8	0.354	0.968
Dy	323	0.195	0.957	-13.1	0.0488	66.3	0.358	0.964
Ho	294	0.178	0.961	-12.8	0.0532	61.0	0.346	0.960
Er	294	0.171	0.963	-12.7	0.0553	59.1	0.355	0.964
Tm	303	0.176	0.964	-12.8	0.0539	59.0	0.372	0.968
Yb	323	0.181	0.960	-12.9	0.0523	60.8	0.395	0.974
Lu	333	0.176	0.966	-12.8	0.0536	62.4	0.389	0.975

Table 8. Coefficient of Langmuir and Freundlich isotherms for lanthanides using *Buccinum tenuissimum* shell biomass after heat-treatment (480°C, 6h)

Furthermore, this result indicates the stronger the monolayer adsorption (the surface adsorption) on the heat-treatment sample relative to on the original sample (before heat-treatment). Judging from the value of R_L or $1/n$ in Table 4, the heat-treatment (480°C) sample also exhibits the favorable property for lanthanides adsorption.

The correlation coefficient (R^2) and other parameters of Langmuir and Freundlich isotherms for lanthanides using “heat-treatment (950°C) sample” is shown in Table 9. It is found that R^2 value for lanthanides in this sample is fairly small compared with the values of “ground original sample” or “heat-treatment (480°C) sample” (In case of La, Ce, Yb and Lu, R^2 can not be estimated due to the lack of sorption data at low initial concentration). The low correlation coefficient (R^2) in this “heat-treatment (950°C) sample” may indicate that the removal of lanthanides occurred not by adsorption mechanism,

	Langmuir					Freundlich		
	a	b	R^2	ΔG_{ads} kJmol ⁻¹	R_L	K_F	$1/n$	
La	—	—	—	—	—	—	—	—
Ce	—	—	—	—	—	—	—	—
Pr	—	—	0.0553	—	—	5690	0.999	0.418
Nd	—	—	0.0727	—	—	10100	1.27	0.375
Sm	—	—	0.00190	—	—	838	0.724	0.157
Eu	—	—	0.2107	—	—	41600	1.65	0.521
Gd	—	—	0.157	—	—	44300	1.69	0.526
Tb	—	—	0.0974	—	—	7980	1.08	0.599
Dy	—	—	0.108	—	—	13900	1.32	0.506
Ho	—	—	0.101	—	—	11100	1.26	0.529
Er	—	—	0.110	—	—	8290	1.14	0.625
Tm	—	—	0.0915	—	—	8830	1.15	0.588
Yb	—	—	—	—	—	—	—	—
Lu	—	—	—	—	—	—	—	—

Table 9. Coefficient of Langmuir and Freundlich isotherms for lanthanides using *Buccinum tenuissimum* shell biomass after heat-treatment (950°C, 6h)

Particularly R^2 value is remarkably small for Langmuir isotherm, and then other relevant parameters can not be estimated. As for Freundlich one, not only R^2 value is relatively small (0.157-0.625), but the value of $1/n$ for most lanthanide is more than unity. That is to say, the almost perfect removal of lanthanides for this sample may be due to other mechanism rather than the adsorption on the biomass. However, the cause or mechanism of lanthanides removal on this sample has yet to be sufficiently clarified in our work, and further investigation to survey the mechanism is needed.

Finally, R^2 and other parameters of Langmuir and Freundlich isotherms for lanthanides using “heat-treatment (950°C) and water added sample” is shown in Table 10. It is found that R^2 value for lanthanides in this sample is fairly large particularly for Langmuir isotherm (0.992-0.999 for Langmuir isotherm and 0.885-0.951 for Freundlich one). This result is similar to that for “heat-treatment (480°C) sample”, and indicates the stronger the monolayer adsorption on this sample. Judging from the value of R_L or $1/n$ in Table10, this sample also exhibits the favorable conditions for lanthanides adsorption.

	Langmuir				Freundlich			
	a	b	R^2	$\Delta G_{\text{ads}}/$ kJmol^{-1}	R_L	K_F	$1/n$	R^2
La	161	0.969	0.999	-17.0	0.0102	59.3	0.264	0.951
Ce	200	0.980	0.999	-17.1	0.0101	70.3	0.283	0.950
Pr	217	0.852	0.998	-16.7	0.0116	69.3	0.327	0.919
Nd	222	0.789	0.997	-16.5	0.0125	68.0	0.340	0.930
Sm	233	0.878	0.996	-16.8	0.0113	72.0	0.364	0.937
Eu	233	0.782	0.996	-16.5	0.0126	68.3	0.380	0.917
Gd	227	0.647	0.997	-16.0	0.0152	61.6	0.384	0.937
Tb	227	0.629	0.996	-16.0	0.0157	61.7	0.390	0.937
Dy	233	0.506	0.996	-15.4	0.0194	57.2	0.409	0.936
Ho	227	0.404	0.996	-14.9	0.0242	50.6	0.425	0.931
Er	222	0.372	0.996	-14.7	0.0262	47.5	0.433	0.928
Tm	233	0.352	0.996	-14.5	0.0276	48.0	0.450	0.922
Yb	244	0.398	0.994	-14.8	0.0245	55.3	0.417	0.934
Lu	217	0.495	0.992	-15.4	0.0198	53.2	0.409	0.885

Table 10. Coefficient of Langmuir and Freundlich isotherms for lanthanides using *Buccinum tenuissimum* shell biomass after heat-treatment (950°C, 6h) and adding water

As mentioned above, biosorption studies have been mainly focused on toxic metals elements such as Cd, Pb, As and Cr so far, and a few reports are focused on lanthanides. The sorption experiments using shell biomass in this work were carried out under low concentration of lanthanide (i.e., 100 cm³ of multi-element standard solution including known initial lanthanide concentration (10 to 500 µg·dm⁻³)). Then, sorption experiment for three lanthanides (La, Eu and Yb) in single component system by this shell biomass is being planned using the solution individually prepared by each nitrate salt: La(NO₃)₃·6H₂O, Eu(NO₃)₃·6H₂O, or Yb(NO₃)₃·3H₂O as the case of seaweed biomass in our work.

4. Conclusion

From this work, it was first quantitatively clarified that seaweed biomass could be efficient sorbents for lanthanides, and exhibit high ability of chemical adsorption. Particularly, *Ulva pertusa* is found to be a promising biosorbent for removing La. It is also suggested that the adsorption on seaweed biomass is mainly due to monolayer sorption because of well-fitting for Langmuir model.

Biosorption characteristic of *Buccinum tenuissimum* shell biomass was also studied for lanthanides. Sorption isotherms were analyzed using Langmuir and Freundlich equations to confirm the efficiency of shell biomass as sorbent. The shell biomass samples showed excellent sorption capacity for lanthanides under our experimental condition, even the presence of diverse ions (Ca²⁺, Mg²⁺, Na⁺ and K⁺) up to the concentration of 200 mg·dm⁻³.

From these results, it was quantitatively clarified to some extent that shell biomass can be an efficient sorbent for lanthanides. It is very significant information from the viewpoint of environmental protection that the shell (usually treated as waste material) can be converted into a biosorbent for lanthanides.

The data obtained and the method used in this work can be useful tool from the viewpoint of resource recovery in future work.

Author details

Naoki Kano

Department of Chemistry and Chemical Engineering, Faculty of Engineering, Niigata University, Japan

Acknowledgement

The present work was partially supported by a Grant-in-Aid for Scientific Research (Research Program (C), No. 22510084) of the Japan Society for the Promotion of Science.

The author wish to express his thanks to Dr. M. Baga of the Marine Ecology Research Institute and Dr. N. Sugai, Dr. H. Handa, Dr. O. Sato and Dr. R. Ishikawa of Niigata Prefectural Fisheries and Marine Research Institute for giving helpful advice concerning sampling, identification and pretreatment of seaweed and shellfish. The author is also grateful to Dr. K. Satoh of Fac. of Sci., Dr. K. Fujii and M. Ohizumi of Office for Environmental and Safety, Mr. N. Saito and Mr. T. Hatamachi of Fac. of Eng. in Niigata University for permitting the use of instrument (ICP-MS, ICP-AES XRD, SEM and Surface Area Analyzer) and facilities and for giving helpful advice in measurement.

5. References

- [1] Saether O. M, Storroe G, Segar. D, Krog R (1997) Contamination of soil and groundwater at a former industrial site in Trondheim, Norway. *Appl. Geochem.* 12:327-332.
- [2] Fu F., Wang Q. (2011) Removal of heavy metal ions from wastewater:A review. *Journal of Environmental Management.* 92:407-418.
- [3] Rahmati M.M., Rabbani P., Abdolali A., Keshtkar A.R. (2011) Kinetics and equilibrium studies on biosorption of cadmium, lead, and nickel ions from aqueous solutions by intact and chemically modified brown algae. *J. Hazard. Mater.* 185: 401– 407.
- [4] Chen J (1997) Batch and continuous adsorption of strontium by plant root tissues. *Bioresource Technology.* 60: 185-189.
- [5] Mohantly K, Jha M, Meikap B C, Biswas M. N (2006) Biosorption of Lanthanides Using Three Kinds of Seaweed Biomasses. *Chem. Eng. J.* 117: 71-77.
- [6] Sudhir D, Tripathi R.M., Hegde A.G. (2008) Biosorption of lead and copper from aqueous solutions by pre-treated crab and arca shell biomass. *Bioresource Technology.* 99: 179-187

- [7] Acosta R I, Rodriguez X, Gutierrez C (2004) Biosorption of chromium (VI) from aqueous solutions onto fungal biomass. *Bioinorganic Chemistry and Application*. 2: 1-7.
- [8] Conard K, Hansen H C B (2007) Sorption of zinc and lead on coir. *Bioresource Technology*. 98: 89-97.
- [9] Sharma P, Kumari P, Srivastava M M, Srivastava. S (2007) Ternary biosorption studies of Cd(II), Cr(III) and Ni(II) on shelled *Moringa oleifera* seeds. *Bioresource Technology*, vol. 98:474-477.
- [10] Dahiya S, Tripathi R M, Hegde A. G (2008) Biosorption of lead and copper from aqueous solutions by pre-treated crab and arca shell biomass. *Bioresource Technology*. 99: 179-187.
- [11] Dahiya S, Tripathi R M, Hegde A G (2008) Biosorption of heavy metals and radionuclide from aqueous solutions by pre-treated arca shell biomass. *Journal of Hazardous Materials*.150:376-386.
- [12] Sari A, Tuzen M (2009) Removal of mercury(II) from aqueous solution using moss (*Drepanocladus revolvens*) biomass: Equilibrium, thermodynamic and kinetic studies. *Journal of Hazardous Materials*. 171: 500-507.
- [13] Sari A, Tuzen M, Mendil D, Soylak M (2009) Biosorptive removal of mercury(II) from aqueous solution using lichen (*Xanthoparmelia conspersa*) biomass: Kinetic and equilibrium studies. *Journal of Hazardous Materials*. 169: 263-270.
- [14] Sari A, Tuzen M (2008) Biosorption of cadmium(II) from aqueous solution by red algae (*Ceramium virgatum*): Equilibrium, kinetic and thermodynamic studies. *Journal of Hazardous Materials*. 157: 448-454.
- [15] Sari A, Tuzen M (2008) Biosorption of Pb(II) and Cd(II) from aqueous solution using green alga (*Ulva lactuca*) biomass. *Journal of Hazardous Materials*. 152:302-308.
- [16] Sari A, Tuzen M (2010) Biosorption of selenium from aqueous solution by green algae (*Cladophora hutchinsiae*) biomass: Equilibrium, thermodynamic and kinetic studies. *Chemical Engineering Journal*. 158:200-206.
- [17] Periasamy K, Namasivayam C (1996) Removal of copper(II) by adsorption onto peanut hull carbon from water and copper plating industry wastewater. *Chemosphere*. 32: 769-789.
- [18] Mevra C. Y, Yusuf K, O. Algur F (2006) Response surface optimization of the removal of nickel from aqueous solution by cone biomass of *Pinus sylvestris*. *Bioresource Technology*. 97:1761-1765.
- [19] Sakao S., Ogawa Y., Uchida H. (1997) Determination of trace elements in sea weed samples by inductively couple plasma mass spectrometry. *Analytica Chimica Acta*. 355: 121-127.
- [20] Fu F., Akagi T., Yabuki S., Iwaki M., Ogura N. (2000) Distribution of rare earth elements in seaweed: implication of two different sources of rare earth elements and silicon seaweed. *Journal of Phycology*. 36: 62-70.
- [21] Punin Crespo M.O., Lage Yusty M. A. (2006) Comparison of supercritical fluid extraction and Soxhlet extraction for the determination of aliphatic hydrocarbons in seaweed samples. *Ecotoxicology and Environmental Safety*. 64: 400-405.
- [22] Cubillas P., Kohler S., Prieto M., Chairat C., Oelkers H. E. (2005) Experimental determination of the dissolution rates of calcite, aragonite, and bivalves. *Chemical Geology*. 216: 59-77.

- [23] Sikes C. S., Wheeler A. P., Wierzbicki A., Dillaman R. M., De Luca L. (1998) Oyster Shell Protein and Atomic Force Microscopy of Oyster Shell Folia. *Biol. Bull.* 194: 304-316.
- [24] Tsui M. T. K, Cheung, K.C, Tam N F Y, Wong M H (2006) A comparative study on metal sorption by brown seaweed. *Chemosphere.* 65:51-57.
- [25] Nader B.,Yadollah Y. (2005) On-line preconcentration of some rare earth elements in water samples using C18-cartridge modified with 1-(2-pyridylazo) 2-naphtol (PAN) prior to simultaneous determination by inductively coupled plasma optical emission spectrometry(ICP-OES). *Analytica Chimica Acta.* 540: 325–332.
- [26] He M., Hu B., Zeng Y., Jiang Z.C. (2005) ICP-MS direct determination of trace amounts of rare earth impurities in various rare earth oxides with only one standard series. *Journal of Alloys and Compounds.* 390: 168–174.
- [27] El-Dessouky S.I., El-Sofany E.A., Daoud J.A. (2007) Studies on the sorption of praseodymium (III), holmium (III) and cobalt (II) from nitrate medium using TVEX-PHOR resin. *Journal of Hazardous Materials.* 143:17-23.
- [28] Sert S., Kutahyali C., Inan S., Talip Z., Cetinkaya B., Eral M. (2008) Biosorption of lanthanum and cerium from aqueous solutions by *Platanus orientalis* leaf powder. *Hydrometallurgy.* 90: 13-18.
- [29] Seki H., Suzuki A. (1998) Biosorption of Heavy Metal Ions to Brown Algae, *Macrocystis pyrifera*, *Kjellmaniella crassifolia*, and *Undaria pinnatifida*. *Journal of Colloid and Interface Science.* 206: 297-301.
- [30] Yang J., Volesky B. (1999) Cadmium Biosorption Rate in Protonated Sargassum Biomass. *Environ. Sci. Technol.* 33: 751-757.
- [31] Diniz V., Volesky B. (2005) Biosorption of La, Eu and Yb using Sargassum biomass. *Water Research,* 39:239-247.
- [32] Sakamoto N., Kano N., Imaizumi H. (2008) Determination of rare earth elements, thorium and uranium in seaweed samples on the coast in Niigata Prefecture by inductively coupled plasma mass spectrometry. *Applied Geochemistry.* 23: 2955-2960.
- [33] Davis T.A., Volesky B., Vieira R.H.S.F (2000) Sargassum seaweed as biosorbent for heavy metals. *Water Research.* 34: 4270-4278.
- [34] Hashim M.A, Chu K.H (2004) Biosorption of cadmium by brown, green, and red seaweeds. *Chemical Engineering Journal.* 97: 249–255.
- [35] Sheng P.X., Ting Y.P., Chen J.P., Hong L. (2004) Sorption of lead, copper, cadmium, zinc, and nickel by marine algal biomass: characterization of biosorptive capacity and investigation of mechanisms. *Journal of Colloid and Interface Science.* 275: 131–141.
- [36] Prieto M, Cubillas P, Fernandez-Gonzalez A (2003) Uptake of dissolved Cd by biogenic and abiogenic aragonite: a comparison with sorption onto calcite. *Geochimica et Cosmochimica Acta.* 67: 3859–3869.
- [37] Bottcher M. E (1997) The transformation of aragonite to $Mn_xCa_{(1-x)}CO_3$ solid-solutions at 20 °C: An experimental study. *Marine Chemistry.* 57: 97-106.
- [38] Kohler S J, Cubillas P, Rodriguez-Blanco J D, Bauer C, Prieto M (2007) Removal of Cadmium from Wastewater by Aragonite Shells and the Influence of Other Divalent Cations. *Environ. Sci. Technol.* 41: 112-118.